Congresso - Stainless Steels-92 - Stockholm, Sweden
Junho 1992

THE EFFECT OF SILICON ON THE LOCALIZED CORROSION BEHAVIOR OF AUSTENITIC STAINLESS STEELS

C.S.C.Machado and L.V.Ramanathan
Instituto de Pesquisas Energeticas e Nucleares,
C.P.11049 Cidade Universitaria, 05508 Sao Paulo. Brazil.

Abstract

Austenitic stainless steels are well known for their excellent general corrosion resistance but exhibit varying resistance to localized corrosion.The influence of adding upto 4.7wt% Si to austenitic Fe18Cr8Ni on the pitting and intergranular (i.g.) corrosion has been studied. The alloys were prepared by vacuum induction melting, annealed at 1300 C and quenched.Some of the specimens were aged at varying temperatures. Pitting tests consisted of prolonged immersion in $FeCl_3$ and anodic polarization measurements in 3.5% NaCl.The addition of upto 4.7wt% Si increased alloy ferrite content to upto 26% and decreased the tendency of the alloy to pit. The pitting potential Ep increased with Si content. Upon aging, the Ep of all the alloys decreased,due mainly to carbide precipitation. Huey tests revealed that in the presence of Si the susceptibility to i.g.corrosion decreased.

Key words:Austenitic stainless steels, silicon, ferrite, pitting, intergranular corrosion.

INTRODUCTION

Austenitic stainless steels (SS) have been widely used due to their excellent mechanical properties and resistance to general aqueous corrosion. They are however susceptible to various forms of localized corrosion such as pitting, crevice and intergranular (i.g.) corrosion. These forms of localized corrosion depend on both environmental factors such as aggressive ion concentration,temperature ,agitation etc. as well as alloy related factors such as composition, microstructure,precipitated phases etc. The addition of certain elements such as Si,Mo,V to austenitic SS stabilizes the ferrite phase and it has been shown that these elements reduce pitting susceptibility (1-3).Wilde found that the addition of upto 4.5% Si to Fe18Cr8Ni SS increased pit initiation resistance by a factor of 20 and crevice corrosion susceptibility to be adversely affected (4). In terms of i.g. corrosion susceptibility, the ferrite phase was found to be beneficial (5). In the presence of Si,significant increase in i.g.corrosion resistance of annealed alloys has been reported (6).The formation of upto 15% ferrite in austenitic SS by plain heat treatment has also been reported to result in improvements in both pitting and i.g. corrosion resistance (7).In order to extend data on the effect of Si addition, and consequently the delta ferrite phase on the localized corrosion of SS, in this paper the

individual and combined influence of Si addition to and heat treatment of AISI 304 on pitting and i.g. corrosion behavior has been reported.

EXPERIMENTAL PROCEDURE

AISI 304 was vacuum induction melted and Si added to it to obtain the 5 alloys with compositions as shown in Table I. Specimens obtained from the alloy ingots were annealed at 1300 C for 1h followed by a water quench. The annealed specimens were subsequently aged at (a) 480 C for 10 and 100h, (b) 600 C for 1 and 20h and (c) 700 C for 1 and 20h. Optical microscopic examination of the specimens was carried out following standard metallographic preparation.

Table I. Chemical composition of experimental alloys.

Alloy	Chemical composition (wt%)										
	C	Mn	P	S	Cr	Ni	Mo	N ppm	Ti	Si	ferrite %
1	0.068	1.38	0.033	0.008	18.23	8.16	0.04	524	0.002	0.62	5.83
2	0.07	1.39	0.019	0.008	19.3	9.0	0.09	532	0.002	0.92	9.90
3	0.067	1.52	0.017	0.007	19.1	9.6	0.09	550	0.003	1.51	10.1
4	0.069	1.53	0.019	0.009	18.9	9.4	0.09	512	0.002	2.46	13.5
5	0.068	1.55	0.02	0.008	18.6	9.1	0.1	521	0.002	4.73	26.00

Two types of pitting tests were carried out. (a) Immersion for 96 h in 10% $FeCl_3$ solution of 0.9 pH at 25 C.Only annealed specimens were tested by this method and pitting corrosion was determined as weight loss. (b) Anodic potentiodynamic polarization measurements in 3.5% NaCl solution at 25 C. A scan rate of 10 mV/s was used and the tests were conducted in a standard corrosion cell with a saturated calomel reference electrode and a Pt counter electrode. Specimens in the different heat treated conditions were polarized from -100 mV to 1000 mV.The pitting potential E_p was determined from the potential vs current density curves. The pitted surfaces of the specimens were examined by optical and scanning electron microscopy. Potentiodynamic reverse scans from -100 mV to +1000 mV to -100 mV were also carried out and the repassivation potential E_{rp} read out from the curves. The difference $E_p - E_{rp}$ for the different alloys was obtained to determine the extent of susceptibility to crevice corrosion (8). The i.g. corrosion behavior of the specimens was determined by

boiling them in 65% HNO_3 for 48h following an initial screening test in oxalic acid. After the test,the specimens were washed, weighed and examined. The extent of i.g. corrosion was determined as mmpy.

RESULTS AND DISCUSSIONS

Microstructural features

The δ ferrite content of the alloys as determined from Shaefflers diagram are shown in Table I. and it can be seen that the ferrite content increased with Si in the alloy.

Optical microscopic examination of the annealed specimens revealed that Alloy 1 had an all austenite structure (fig. 1).Comparison of the structures of Alloys 2-4 shows that with increasing Si, the ferrite grains increased in size from being spots to large coalesced particles. Alloy 5 had an all ferrite structure with a fine distribution of carbides (fig. 2). This structure results because the position of this alloy (at 1300 C) in the phase diagram shifts to the single phase ferrite field and is retained upon quenching.The fine carbides in the ferrite matrix result due to the low solubility of C in δ ferrite.Aging of the alloys at 480 C for 10h did not cause significant changes in the microstructures. Alloys 4 and 5 revealed $M_{23}C_6$ carbides at δ / γ and δ / δ grain boundaries. A precipitate free zone close to the g.b was also observed in Alloy 5 (fig.3). Increasing the time at 480 C resulted in decrease in the total amount of ferrite in Alloys 1-4. Aging at 600 C for 2h revealed fine carbide precipitates at the g.b in Alloy 1 and coalesced ferrite in the two low Si alloys.Alloys 4 and 5 revealed $M_{23}C_6$ at the γ /δ and δ/δ boundaries. Upon increasing the aging time at 600 C, most carbides precipitated both at g.b and within the ferrite grains (fig.4). Increasing the aging temperature to 700 C or time at this temperature resulted in very large amounts of carbide precipitates at g.b, or within the ferrites and a clear delineation of depleted zones near g.b.

Localized corrosion behavior

The pitting corrosion rates of the different alloys as deterimined from the $FeCl_3$ immersion tests are shown in figure 5. The pitting rate decreased with Si content and this decrease is more pronounced as the solution volume to specimen area ratio increased. The extent to which pitting rate decreased with Si content upto 4.5wt% although significant, is not as high as reported elsewhere (4). The low corrosion rates at low solution volume to specimen area ratios may be attributed to early saturation of the solution with complexed metal chlorides. The results of the optical microscopic examination of the pitted surfaces are summarized in Table II.
The anodic polarization curves of the various annealed alloys in 3.5% NaCl are shown in fig.6. In the curves the pitting potential

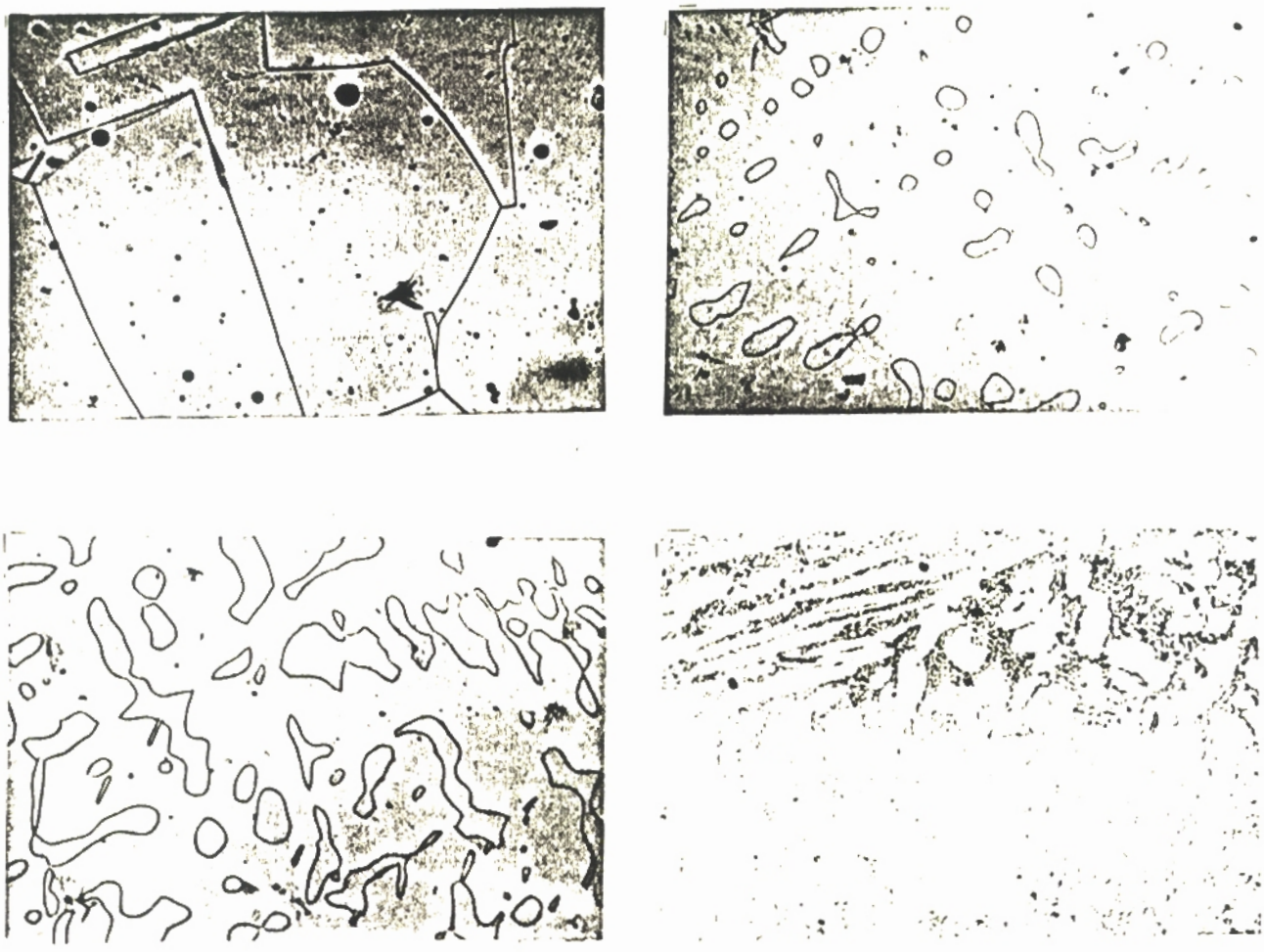

Figure 1. Optical micrographs of alloys annealed at 1300 C (a) Alloy 1,(b) Alloy 2, (c) Alloy 3,(d) Alloy 4. 200X

Figure 2. Optical micrograph of Alloy 5 annealed at 1300 C. 200X

E_p is characterized by an increase in current density (c.d).The variation in E_p with alloy composition and heat treatment is shown

in Table III. E_p of the annealed alloys increased with Si content.However upon aging at 480 C for 10h the E_p of all the alloys decreased. Further increase in aging time at 480 C or in aging temperature resulted in decrease of E_p.The decrease in E_p

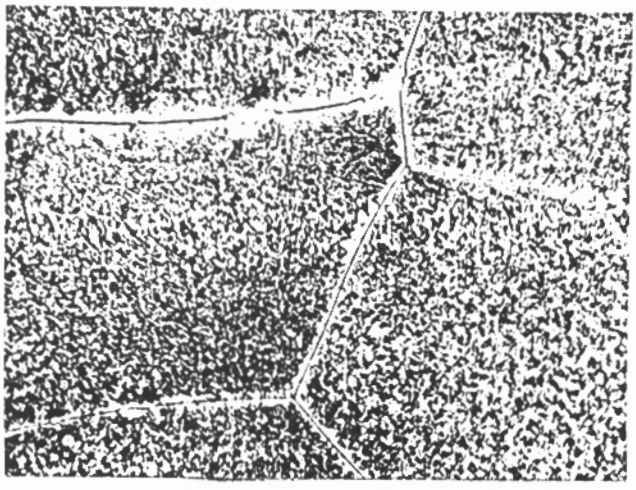

Figure 3. Optical micrograph of Alloy 5 aged at 480 C for 10h. 200X

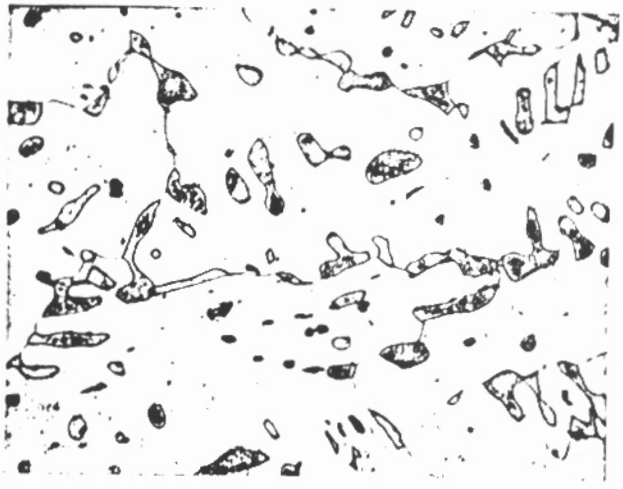

Figure 4. Optical micrograph of Alloy 5 aged at 600 C for 20h. 200X

Table II. Surface features following pitting test in $FeCl_3$.

Alloy	Description
1	Various large pits 1-3mm close to each other forming craters and fine pits over rest of the surface.
2	Various large pits (1-3mm) and some very fine pits.
3	Some medium sized pits (1-2mm) and few small pits.
4	Some medium sized pits (1-2mm) and few small pits.
5	Very few small pits (0.5 - 1mm).

indicates the alloys increasing propensity to pit.This results from decrease in ferrite content and increase in carbide precipitates as the alloys are aged.Nevertheless, in any heat treated condition, the E_p increased with Si content of the alloy. Table IV gives E_p, E_{rp} and $(E_p - E_{rp})$ for the various alloys.The value $(E_p - E_{rp})$, considered to be indicative of the possible extent of crevice corrosion, increases with Si content of the

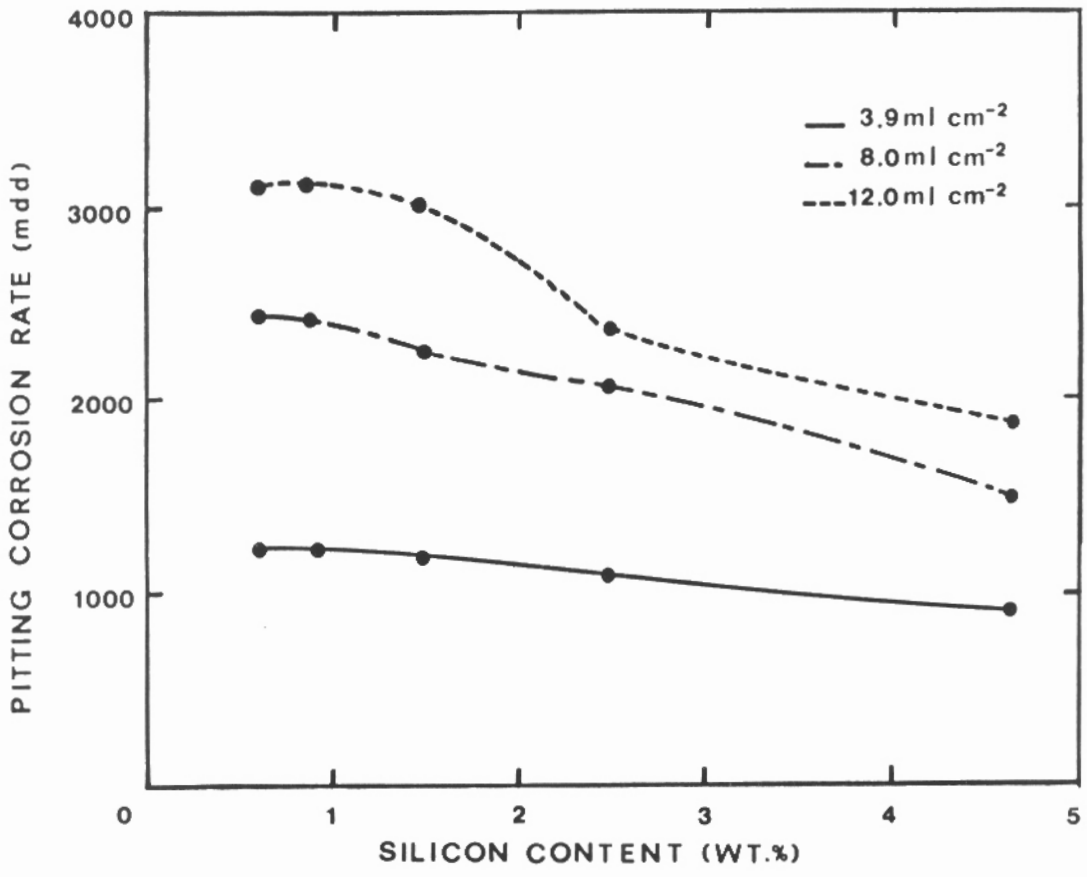

Figure 5. Pitting corrosion rate in 10% $FeCl_3$ aas a function of Si content in the experimental alloys.

alloys. These observations are in agreement with data reported elsewhere (4).

The results of the i.g. corrosion tests are shown in Table V. Alloys 1-4 in the annealed condition were not susceptible as determined by the oxalic acid test. Alloy 5 was severely corroded and this could be attributed to the Cr depleted zones resulting from $M_{23}C_6$ precipitation in the ferrite matrix. Upon aging this alloy, the extent of i.g. corrosion decreased, but remained high, due mainly to the precipitates that were observed at or near the δ/δ or γ/δ g.b. Comparison of the i.g. corrosion rates of the othere alloys in the aged conditions revealed that when aged at 600 C for 10h alloys 1 and 2 underwent complete sensitization, whereas alloys 3 and 4 which have a higher Si content exhibited reduced susceptibility.The decrease in susceptibility of alloys aged at 700 C may be due to the temperature being above the sensitization zone in the TTT diagram of these alloys. Partial susceptibility may have resulted from the short permanance of these alloys in the sensitization zone during cooling.

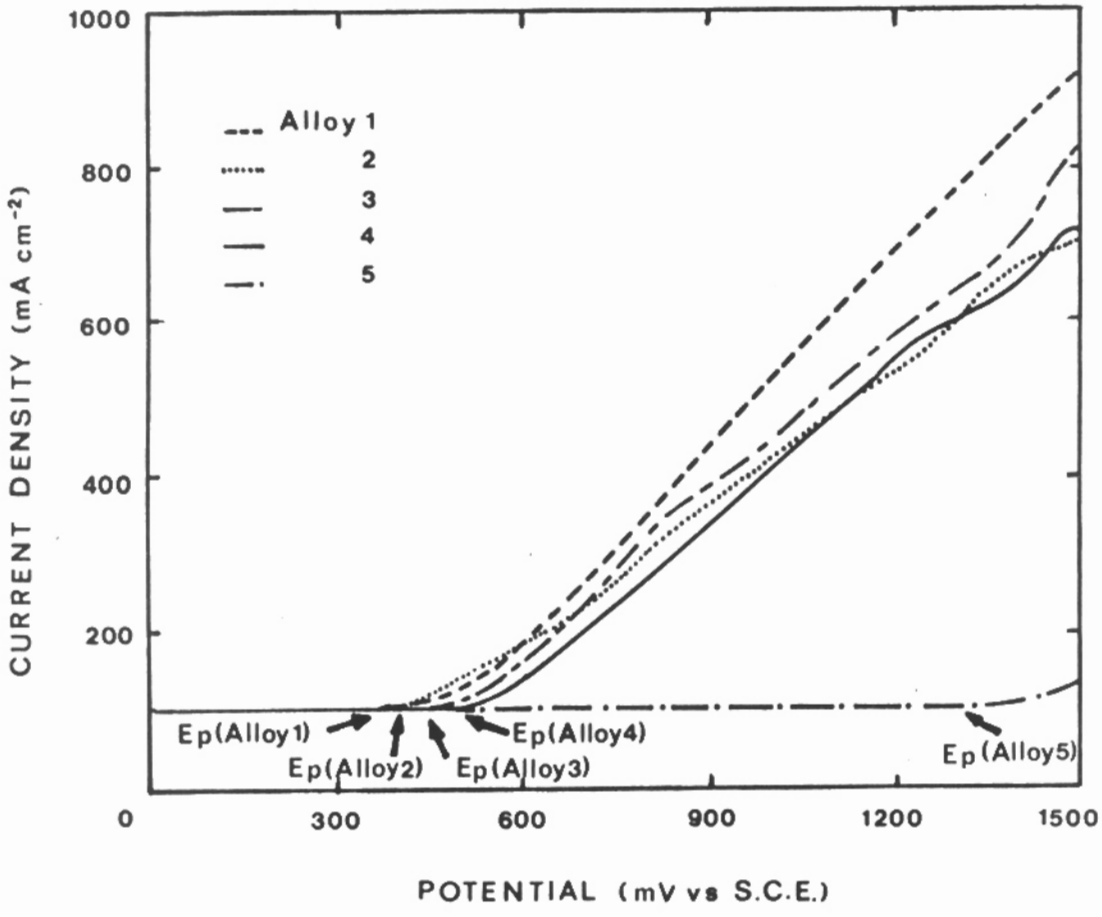

Figure 6. Anodic polarization curves of Si containing stainless steels in 3.5% NaCl at 25 C.

General discussions

The amount of δ ferrite in the alloys increased with Si content. Upon heat treatment, depending on the alloy and aging conditions, the δ phase transformed to γ and $M_{23}C_6$. In chloride ion environments all the alloys pitted. However the pitting potential, pit nucleation sites and number of pits varied with alloy composition and heat treatment. In the annealed alloys,the pits nucleated in the γ and the δ phase as observed from SEM/EDAX studies (fig.7). In the aged alloys,regions in the vicinity of $M_{23}C_6$ or near g.b were sites for pit nucleation.The pitting potential increased in the presence of Si. Since pitting occures at sites where the passive film is ruptured by the aggressive ions, the higher E_p of the Si containing alloys can be attributed to the formation of a more continuous and nearly defect free film of just Cr_2O_3 or Cr_2O_3 and SiO_2 on the ferrite phase. The formation of $M_{23}C_6$ and γ in the aged alloys results in the Cr

Table III. Pitting potentials of experimental alloys in different heat treated conditions in 3.5% NaCl at 25 C.

Heat treatment		Pitting potential mV vs SCE				
		Alloy 1	Alloy 2	Alloy 3	Alloy 4	Alloy 5
1300 C,1h,q		437	494	654	>1500	>1500
1300 C 1h qnch aged at	480 C 10h	424	460	643	920	>1500
	480 C 100h	389	389	566	1094	>1500
	600 C 1h	270	265	552	653	921
	600 C 20h	204	298	471	576	954
	700 C 1h	241	310	471	617	1113
	700 C 20h	204	208	497	508	835

Table IV Pitting and repassivation potentials of the alloys in aerated 3.5% NaCl. Scan rate 10mVs^{-1}

Alloy	Pitting Potential (mV) E_p	Repassivation potential (mV) E_r	$E_p - E_r$ (mV)
1	221	-10	231
2	252	-29	281
3	405	-20	425
4	476	-10	486
5	>1000	---	---

Table V. Intergranualar corrosion rate of the experimental alloys as determined by HUEY test.

Heat treatment		Corrosion rate in mmpy of Alloys				
		1	2	3	4	5
1300 C	1h,qnch	--	--	--	--	1.21
1h qnch aged at	480-10h	--	--	--	--	1.33
	480-100h	--	--	--	--	1.68
	600-1h	--	--	--	--	0.76
	600-20h	1.44	0.77	0.16	0.21	0.56
	700-1h	0.17	0.20	--	--	0.60
	700-20h	0.21	0.17	0.18	0.17	0.58

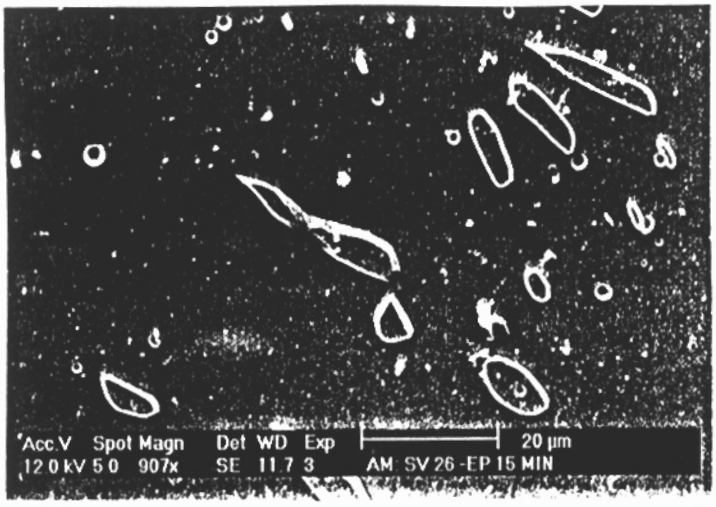

Figure 7. Scanning electron micrograph of Alloy 4 polarized in 3.5% NaCl at E_p for 15 minutes.

depleted zones.Consequently,the oxides formed on these zones are defective and become sites for pit initiation. The i.g. corrosion susceptibility of the silicon containing alloys depends to a large extent on the position of the aging conditions with respect to the sensitization zone in the TTT diagrams of the alloys and the i.g corrosion behavior is probably controlled by silica film formation.

REFERENCES

1. Tomashov, N.D., Chernova, O.P., and Markova, O.N., Corrosion, vol.20, 5, 1964, 166t.

2. Truman, J.E., "Corrosion, Metal/Environment Reactions," Shreir, L.L., Ed., Vol.1, Newnes Butterworths, London, 1976, 331.

3.Sedriks, A.J., Corrosion of Stainless Steels, John Wiley and Sons, Inc, New York, NY, 1979.

4. Wilde, B.E., Corrosion, 42, 3, 1986, 147.

5. Wilde, B.E.,Weber, J.E., Brit, Corros. J.,4, 1969, 42.

6. Wilde, B.E., Corrosion, 44, 10, 1988, 699.

7. Devine, T.M., J.Echem. Soc., 126, 3, 1979, 374.

8. Wilde, B.E.,Corrosion, 28,8,1972,283.